Published in final edited form as:
Nature. 2010 October 21; 467(7318): 972–976. doi:10.1038/nature09421.

Oxidative stress induces angiogenesis by activating TLR2 with novel endogenous ligands

Xiaoxia Z. West[1,2,*], **Nikolay L. Malinin**[1,*], **Alona A. Merkulova**[1], **Mira Tischenko**[1], **Bethany A. Kerr**[1], **Ernest C. Borden**[3], **Eugene A. Podrez**[1], **Robert G. Salomon**[2], and **Tatiana V. Byzova**[1,3]

[1] Department of Molecular Cardiology, JJ Jacobs Center for Thrombosis and Vascular Biology, NB50, The Cleveland Clinic Foundation, 9500 Euclid Ave, Cleveland, OH 44195

[2] Department of Chemistry, Case Western Reserve University, Cleveland, OH 44106

[3] Taussig Cancer Institute, The Cleveland Clinic Foundation, 9500 Euclid Ave, Cleveland, OH 44195

Abstract

Reciprocity of inflammation, oxidative stress and neovascularization is emerging as an important mechanism underlying numerous processes from tissue healing/remodeling to cancer progression[1,2]. Whereas the mechanism of hypoxia-driven angiogenesis is well understood[3,4], the link between inflammation-induced oxidation and de novo blood vessel growth remains obscure. Here we show that the end products of lipid oxidation, ω-(2-carboxyethyl)pyrrole (CEP) and other related pyrroles[5], are generated during inflammation and wound healing and accumulate at high levels in aging tissues and in highly vascularized tumors. The molecular patterns of carboxyalkylpyrroles are recognized by Toll-like receptor 2 (TLR2), but not TLR4 nor scavenger receptors on endothelial cells (ECs), leading to a VEGF-independent angiogenic response. CEP promoted angiogenesis in hind limb ischemia and wound healing models through TLR2 signaling in a MyD88-dependent manner. Neutralization of endogenous carboxyalkylpyrroles impaired wound healing and tissue re-vascularization and diminished tumor angiogenesis. Both TLR2 and MyD88 are required for CEP-induced stimulation of Rac1 and endothelial migration. Together, these findings establish a new function of TLR2 as a sensor of oxidation-associated molecular patterns, providing a key link connecting inflammation, oxidative stress, innate immunity and angiogenesis.

Angiogenesis can either promote host defense and tissue repair or exacerbate organ dysfunction resulting in disease. In many pathologies, angiogenesis and inflammation[6] are intimately related. Inflammatory cells release proangiogenic growth factors, including VEGF[7], which facilitate neovascularization. Newly-formed blood vessels enhance inflammatory cell recruitment, thereby promoting chronic inflammation. Leukocytes, in particular myeloid cells, are guided by[8] and contribute to[9] oxidative stress and the

Correspondence and requests for material should be addressed to T.V.B (byzovat@ccf.org).
*These authors contributed equally to this work.

Supplementary Information accompanies the paper on www.nature.com/nature.

Author contributions N.L.M., E.A.P., and T.V.B. designed experiments. *In vivo* and *ex vivo* experiments were performed by X.Z. with a help from A.A.M. and M.T. *In vitro* experiments were performed by with help from B.A.K. Melanoma samples and their analysis was done by E.C.B. Synthesis of CAPs was performed by R.G.S. The data were analyzed and plotted by X.Z. The manuscript was written by N.L.M. and T.V.B..

Author Information Reprints and permissions information is available at www.nature.com/reprints. The authors declare no competing financial interests.

generation of oxidative products, including hydroxy-ω-oxoalkenoic acids and their esters (Supplementary Fig. 1). When present in oxidized phospholipids, these molecules are recognized by the scavenger receptor CD36 and contribute to atherosclerotic progression and platelet hyper-reactivity[10,11]. Hydrolysis followed by reaction of the resulting unesterified hydroxy-ω-oxoalkenoic acids with proteins, or reaction of the esterified hydroxy-ω-oxoalkenoic acids with proteins followed by hydrolysis, gives rise to a family of carboxyalkylpyrrole protein adducts (CAP), among them CEP and similarly-modified compounds (Supplementary Fig. 1). These adducts, present in oxidized LDL, accumulate in atherosclerotic plaques and are found in the retina[12], where they promote choroidal neovascularization and age-related macular degeneration[5,13].

These adducts, CEP in particular, are transiently present during wound healing, reaching a maximum 3d after injury before returning to original levels when the wound is healed (Fig. 1a,b and Supplementary Fig. 2a–c). This increase coincides with the recruitment of bone marrow-derived cells (Supplementary Fig. 2b), which generate additional oxidants[9]. A substantial proportion of CEP (~60% at 3d, ~50% at 7d) is present in F4/80^{+} macrophages (Fig. 1c) but not in Gr-1^{+} neutrophils (Supplementary Fig. 2c). High levels of CEP coincide with intense wound vascularization, suggesting a role for CEP in wound angiogenesis (Fig. 1a,b). In contrast to wounds, CEP levels were continuously elevated in pathological states. In melanoma, exhibiting excessive vascularization and inflammation (assessed by CD31 and CD68 staining, respectively), CEP levels were elevated 6-fold (Fig. 1d). Likewise, in murine melanoma, CEP levels were elevated 9-fold (Supplementary Fig. 3). In contrast to wound and tumor tissues, CEP in uninjured muscle was confined to arteriolar smooth muscle cells (Fig. 1e). Notably, CEP accumulation increased in aging tissues (Fig. 1f). These data suggest a role of CEP in inflammation-associated vascularization.

When tested on ECs from human umbilical vein, mouse lung or aorta, CEP had proangiogenic effect comparable to VEGF, as evaluated in various assays (Fig. 2, Supplementary Fig. 4 and S5). Similar to VEGF, the effect of CEP was integrin-mediated (Supplementary Fig. 5b). The proangiogenic effect was dependent on the presence of pyrrole adducts, and the protein moiety did not influence CEP's effect, as adducts coupled to MSA, HSA or a dipeptide were equally effective (Fig. 2a and Supplementary Fig. 4).

However, in contrast to VEGF, stimulation of ECs with CEP did not result in VEGFR2 phosphorylation (Supplementary Fig. 6). Moreover, CEP-induced effects both *in vitro* and *in vivo* were not reduced by the VEGFR kinase inhibitor AAL-993[14] at the concentration sufficient to block VEGF-A effects (Fig. 2b,c), vehicle alone having no effect (data not shown). In a wound healing assay, CEP accelerated vascularization and wound closure; this effect was unimpeded by AAL-993 which delayed wound closure in control animals (Fig. 2d). Thus, CEP activates the proangiogenic responses independently of VEGF/VEGFR2 signaling. Adducts from the same family of CAPs (Supplementary Fig. 1), represented by CPP (carboxypropylpyrrole), were also proangiogenic (Fig. 2a, Supplementary Fig. 4a,b, and 5a), indicating that the ECs respond to the molecular pattern rather than to a particular chemical moiety.

To identify receptors mediating CEP-induced angiogenesis, we tested the role of CD36 and SR-BI scavenger receptors, as CD36 recognizes precursors of CAPs[11]. Both CEP and CPP adducts were as effective on CD36$^{-/-}$ and SR-BI$^{-/-}$ ECs as on wild type cells (Supplementary Fig. 7a–d), indicating that scavenger receptors are not involved in recognition of these adducts.

Since ECs respond to CAP's molecular pattern, which is a characteristic feature of oxidative stress, we hypothesized the involvement of Toll-like family receptors (TLRs) in CEP-

induced angiogenesis. TLRs recognize a number of damage associated molecular patterns including pathogen-associated molecular patterns (reviewed in[15,16]) and ligands of host origin[17–22], contributing to immune defense and to sterile inflammation, respectively. We focused on TLR2 and TLR4 since they are expressed on the endothelium, are implicated in angiogenesis[23] and are known to recognize a broad range of protein and lipid ligands[24]. Anti-TLR2, but not TLR4 antibodies, inhibited CEP-, but not VEGF-induced, tube formation (Fig. 2e) and EC migration (Supplementary Fig. 8a). To further address the role of TLR2 in CEP-driven angiogenesis, ECs from $TLR2^{-/-}$ mice were compared to $TLR2^{+/+}$ controls. $TLR2^{-/-}$ ECs did not respond to CEP or CPP treatment in a number of *in vitro* assays; in contrast, VEGF-triggered responses were not affected by the lack of TLR2 (Fig. 2f, Supplementary Fig. 8b and 9a). To confirm the role of TLR2 in EC proangiogenic responses, we tested the TLR2 synthetic ligand Pam3CSK4[25]. This ligand induced robust sprouting of EC from aortic rings of $TLR2^{+/+}$ but not $TLR2^{-/-}$ mice (Fig. 2g). Pam3CSK4 was as effective as CEP or VEGF in tubulogenesis and cell adhesion assays, and the effect of Pam3CSK4 was eliminated by TLR2 antibodies (Supplementary Fig. 9b and 10a). To investigate the relative roles of CEP and VEGF, we examined the effect of a VEGF2 inhibitor, AAL-993, or TLR2 deletion in wound healing. Inhibiting either pathway had a similar effect and in combination led to additive inhibition of wound closure (Supplementary Fig. 10b).

Having established the role of TLR2 in the proangiogenic effects of CEP on ECs, we hypothesized that CEP administration might promote vascularization in ischemic or injured tissues. In a hind limb ischemia model, CEP-dipeptide injections resulted in 11-fold increase of the pyrrole adduct in muscle tissue (Supplementary Fig. 11a), which promoted re-vascularization of the ischemic limb (Fig. 3a) and restructuring of collateral blood vessels bypassing the ligated femoral artery (Supplementary Fig. 11b). Exogenous CEP affected vascularization in a TLR2-dependent manner (Fig 3a). Consequently, CEP injection increased blood flow in $TLR2^{+/+}$ but not $TLR2^{-/-}$ mice (Fig. 3b). In a wound model, exogenous CEP accelerated wound closure and vascularization in $TLR2^{+/+}$ but not $TLR2^{-/-}$ mice (Fig. 3c). Moreover, tumors implanted in $TLR2^{-/-}$ mice exhibited dramatically decreased vascularization and increased areas of necrosis (Supplementary Fig. 12).

To distinguish the effect of CEP on ECs from that on leukocytes, $TLR2^{+/+}$ and $TLR2^{-/-}$ mice were transplanted with $TLR2^{+/+}$ bone marrow. In wound assays, CEP injection into $TLR2^{+/+}$ >$TLR2^{+/+}$ chimeras accelerated wound closure, whereas $TLR2^{+/+}$ >$TLR2^{-/-}$ animals healed slower, and CEP had no effect on wound closure (Fig. 3d). The difference was associated with a 2.5-fold increase in vasculature by CEP treatment of $TLR2^{+/+}$ but not $TLR2^{-/-}$ host animals (Fig. 3e). Even in the absence of exogenous CEP, vascular area was diminished in wounds of $TLR2^{+/+}$ >$TLR2^{-/-}$ chimeras as compared to $TLR2^{+/+}$ >$TLR2^{+/+}$ (Fig. 3f). Moreover, melanoma vascularization in $TLR2^{+/+}$ >$TLR2^{-/-}$ animals was reduced relative to $TLR2^{+/+}$ >$TLR2^{+/+}$ or $TLR2^{-/-}$ >$TLR2^{+/+}$ chimeras (Fig. 3g). Thus, TLR2 on non-hematopoietic cells mediated vascularization induced by exogenous CEP and it also contributed to wound and tumor angiogenesis in the absence of an exogenous adduct.

Since CEP is accumulated at high levels during wound healing (Fig. 1 and Supplementary Fig. 2) and in tumors (Fig. 1d and Supplementary Fig. 3), we addressed the contribution of endogenously generated adducts to the process of vascularization in these models. Intravenous administration of neutralizing antibodies to CEP[13], but not control antibodies, resulted in a more than 2-fold reduction of wound recovery (Fig. 4a). Vascularization of wounds was also inhibited by anti-CEP but not control antibodies, demonstrating the significance of endogenously generated CEP in wound angiogenesis (Fig. 4b and Supplementary Fig. 13). Remarkably, administration of anti-CEP, but not control antibodies, diminished progression and vascularization of melanoma and this effect was additive to that

of the VEGFR inhibitor (Fig. 4c). Thus, the CEP/TLR2 axis drives VEGF-independent angiogenesis in a variety of pathological conditions.

The key mechanism underlying the broad ligand specificity of TLR2[24] is its heterodimerization with other members of the TLR family, particularly TLR1 and TLR6[26]. In a tube formation assay, anti-TLR1 and anti-TLR2, but not anti-TLR6 blocking antibodies, diminished the CEP-induced angiogenic response (Fig. 4d), indicating the involvement of TLR2/TLR1 heterodimers in CEP recognition. It appears that CEP directly interacts with TLR2, since recombinant TLR2 bound the CEP protein adduct but not the carrier protein alone (Supplementary Fig. 14a). Similar to other TLR2 ligands, CEP stimulated NF-κB in a cell-based assay (Supplementary Fig. 14b).

Next, we evaluated the role of MyD88, a mediator of TLR2 signaling, in the proangiogenic activity of CEP. CEP-induced EC sprouting is MyD88-dependent since MyD88$^{-/-}$ cells did not respond to stimulation by CEP (Fig. 4e). VEGF-induced angiogenesis was not affected by the lack of MyD88 (Fig. 4e). Considering that CEP-induced angiogenesis is integrin-dependent, we focused on mediators of integrin and TLR signaling. Rac1 mediates integrin-dependent migration in vascular development[27] and is reported to be activated downstream of TLRs[28]. Accordingly, we assessed Rac1 GTP-loading in response to CEP treatment. GTP-bound Rac1 is increased by CEP treatment of TLR2$^{+/+}$, but not TLR2$^{-/-}$ nor MyD88$^{-/-}$ cells (Fig. 4f). Thus, lipid oxidation products, represented by CEP, promote the angiogenic responses of ECs by activating TLR2 signaling in a MyD88-dependent manner, resulting in Rac1 activation, which, in turn, facilitates integrin function.

Altogether our results establish a novel mechanism of angiogenesis that is independent of hypoxia-triggered VEGF expression. The products of lipid oxidation are generated as a consequence of oxidative stress and are recognized by TLR2, possibly in a complex with TLR1 on ECs, and promote angiogenesis *in vivo*, thereby contributing to accelerated wound healing and tissue recovery. If high levels of CEP and its analogs accumulate in tissues, it may lead to excessive vascularization, e.g. in tumors. Contribution of the CEP/TLR2 axis to angiogenesis varies in different physiological settings possibly depending on the extent of oxidative stress. CEP-driven angiogenesis may be an attractive therapeutic target, especially in cancers resistant to anti-VEGF therapy. Inflammation and oxidation-driven angiogenesis may occur in other pathologies, for example atherosclerosis, where arterial thickening can depend on its microvasculature. In these settings, there is an extensive generation of oxidative products which might promote atherogenesis via TLR2. Indeed, it was shown that TLR2$^{-/-}$ mice are protected from atherosclerosis, and this effect could be mediated by cells other than bone marrow-derived[29]. Thus, along with pathogen- and danger-associated molecular patterns, TLR2 recognizes an oxidation-associated molecular pattern. This new function of TLR2 as a sensor of oxidative stress reveals the shortcut link between innate immunity, oxidation and angiogenesis.

Methods summary

Immunostaining was completed to assess the presence of endogenous CEP in various tissues. Tube formation assays, matrigel plug assays, wound healing assays, aortic ring assays, tumor implantation models, and a hind limb ischemia model evaluated the angiogenic effects of CEP and TLR2. TLR2$^{+/+}$ and TLR2$^{-/-}$ mice were used for the above assays and in bone marrow transplantation studies. MyD88$^{-/-}$ mice and a commercially available Rac1 activation assay were used to examine the CEP/TLR2 signaling pathway.

Methods

Animal studies

Wild type C57BL/6 and DsRed transgenic mice were obtained from Jackson Laboratory, $CD36^{-/-}$ from Dr. M. Febbraio (Cleveland Clinic), $SR\text{-}BI^{-/-}$ from Dr. M. Krieger (Massachusetts Institute of Technology), $MyD88^{-/-}$ and $TLR2^{-/-}$ from Dr. S. Akira (Osaka University). All mice were maintained in the Biological Resources Unit of the Lerner Research Institute, accredited by the Association for the Assessment and Accreditation of Laboratory Animal Care International. All experimental work was conducted in compliance with the Institutional Animal Care and Use Committee program.

Immunohistochemistry and image analysis

For immunofluorescence staining, we used rabbit polyclonal anti-CEP (described in[5]), anti-CD31 (BioLegend), anti-αSMA (Rockland), anti-CD68 (BD Biosciences) antibodies. We embedded samples in OCT freezing medium and prepared 7μm thick tissue sections. Sections were fixed in 4% paraformaldehyde. After incubation with primary antibodies, samples were washed with PBS and exposed to a Alexa Fluor-labeled secondary antibody, either goat anti-rabbit Alexa Fluor488, anti-rat Alexa Fluor568, or anti-mouse Alexa Fluor568 (Invitrogen). The slides were mounted with medium (DakoCytomation) and images were taken by either a TCS-SP (Leica) or a ZMZ1000 (Nikon) microscope. For quantification, the images were analyzed with ImagePro software (Media Cybernetics).

Bone marrow transplant (BMT) and wound assay

We performed BMT as previously described[30]. Briefly, we subjected two month old male wild type $TLR2^{+/+}$ or $TLR2^{-/-}$ mice to irradiation with a total dose of 9 Gy followed by bone marrow reconstitution by tail vein injection with 10^7 bone marrow cells isolated from donor femurs. Eight weeks after BMT, mice were used for wound healing assays. A back punch wound healing model was used as described elsewhere[31]. Where indicated, mice were given CEP-dipeptide (M.W. 381.42) s.c injections (1.4 μg per g of body weight) at the time of injury and on days 2, 4, and 6. Separately, control mice were subjected to a back punch and injected s.c. with CEP-dipeptide (30 μg) and AAL-993 (13 nmol) every other day within 1 cm of the wound edge.

Aortic Ring Assay

The mouse aortic ring assay was performed as previously described[32]. Aortic rings were treated with CEP-dipeptide (0.5 μg/ml), VEGF (60 ng/ml) or Pam3CSK4 (300 nM).

Isolation of Endothelial cells

Mouse lungs were excised, minced, and digested using a collagenase-dispase reagent (Roche Diagnostic). Digests were strained and the resulting cell suspension was plated on flasks coated with 10 μg/ml fibronectin. Thereafter, endothelial cells were isolated and characterized as described previously[32].

Tube formation assay

HUVEC or MLEC cells were seeded on Matrigel-coated plates (BD Bioscience). Medium was supplemented with VEGF (60 ng/ml) or protein adducts (0.5 μg/ml) as indicated, and cells were further incubated at 37°C for 8h. Anti-TLR2 blocking (developed by Dr. Salomon), anti-TLR4 blocking (BioLegend) and isotype control antibodies (IgG2a, BioLegend) or anti-TLR1 and anti-TLR6 blocking antibodies (InVivoGen) were added at 15 μg/ml at the beginning of the experiment. Alternatively, we incubated cells with 100 nM AAL-993 (Enzo Life Sciences). Tube formation was observed using a phase contrast

inverted microscope, and photographs were taken from each well. The data were quantified by measuring the length of tubes with ImagePro software.

Matrigel plug assay

Matrigel (500μl) containing AAL-993 (200 nM) in combination with VEGF (250 ng) or CEP-dipeptide (10 μg/ml) was injected s.c. into C57BL/6 mice. Plugs were removed after 7 days and sectioned.

Hind limb ischemia model

The femoral artery was ligated near the caudally branching deep femoral artery and a second ligation was placed in proximity of the tibial artery branching. The portion of the artery and vein between the ligation points was excised. CEP-dipeptide was administered as PBS solution (1.4 μg per gram of body weight) injected intramuscularly distal to the ligation site, with injections every 48 hrs starting at the day of operation. Intramuscular CEP content was evaluated by immunohistochemistry and quantified using ImagePro software. Hind-limb blood flow was measured by a laser Doppler moorLDI2-IR near infra-red laser Class 3R (Moor Instruments) in arbitrary perfusion units (PU). The results were plotted as a ratio of operated to non-operated leg for each animal to account for variations between animals.

Tumor implantation

B16-F10 murine melanoma cells (ATCC) were injected subcutaneously (1.25×10^6 cells per injection) in wild type or BMT animals as indicated. Tumors were analyzed at day 10 post implantation. Mice were injected i.p. with AAL-993 (25 μmol), anti-CEP antibody (5 μg per gram body weight), or isotype control (IgG2a, 5 μg per gram body weight).

Rac1 activation assay

Per assay, we used 2×10^6 cells lysed in 500 μl buffer: 25 mM HEPES KOH pH 7.5, 250 mM NaCl, 1% NP-40, 10% glycerol, 10 mM MgCl2 2 mM EGTA. GST-PAK-PBD pre-absorbed on glutathione agarose beads (Cytoskeleton) was added in the amount of 20 μl 50% slurry followed by incubation on a rotary shaker for 45 min at 4°C. Beads were washed four times with lysis buffer before elution with SDSPAGE sample buffer. Rac1 was detected by Western Blot (clone 102, BD Bioscience).

Statistical analysis

All data are presented as mean ± s.e.m.. Probability values were based on a paired t test: NS represents not significant, * $p<0.05$, ** $p<0.01$, *** $p<0.001$.

Supplementary Material

Refer to Web version on PubMed Central for supplementary material.

Acknowledgments

This work was supported by NIH grants to T.V.B., E.A.P. and R.G.S. and an American Heart Association grant 10SDG4300062 to N.L.M. We express our gratitude to L. Hong for the help with synthesis of CEP and CPP adducts, Y. Cui for expressing and purifying anti-CEP monoclonal antibodies, and J. Crabb for providing anti-CEP mAb hybridoma cells.

References

1. Jackson JR, Seed MP, Kircher CH, Willoughby DA, Winkler JD. The codependence of angiogenesis and chronic inflammation. FASEB J 1997;11 (6):457–465. [PubMed: 9194526]

2. Coussens LM, Werb Z. Inflammation and cancer. Nature 2002;420 (6917):860–867. [PubMed: 12490959]
3. Mazzone M, et al. Heterozygous deficiency of PHD2 restores tumor oxygenation and inhibits metastasis via endothelial normalization. Cell 2009;136 (5):839–851. [PubMed: 19217150]
4. Fraisl P, Mazzone M, Schmidt T, Carmeliet P. Regulation of angiogenesis by oxygen and metabolism. Dev Cell 2009;16 (2):167–179. [PubMed: 19217420]
5. Crabb JW, et al. Drusen proteome analysis: an approach to the etiology of age-related macular degeneration. Proc Natl Acad Sci U S A 2002;99 (23):14682–14687. [PubMed: 12391305]
6. Karin M, Lawrence T, Nizet V. Innate immunity gone awry: linking microbial infections to chronic inflammation and cancer. Cell 2006;124 (4):823–835. [PubMed: 16497591]
7. Martin P. Wound healing--aiming for perfect skin regeneration. Science 1997;276 (5309):75–81. [PubMed: 9082989]
8. Niethammer P, Grabher C, Look AT, Mitchison TJ. A tissue-scale gradient of hydrogen peroxide mediates rapid wound detection in zebrafish. Nature 2009;459 (7249):996–999. [PubMed: 19494811]
9. Segal AW. How neutrophils kill microbes. Annu Rev Immunol 2005;23:197–223. [PubMed: 15771570]
10. Podrez EA, et al. Identification of a novel family of oxidized phospholipids that serve as ligands for the macrophage scavenger receptor CD36. J Biol Chem 2002;277 (41):38503–38516. [PubMed: 12105195]
11. Podrez EA, et al. Platelet CD36 links hyperlipidemia, oxidant stress and a prothrombotic phenotype. Nat Med 2007;13 (9):1086–1095. [PubMed: 17721545]
12. Gu X, et al. Carboxyethylpyrrole protein adducts and autoantibodies, biomarkers for age-related macular degeneration. J Biol Chem 2003;278 (43):42027–42035. [PubMed: 12923198]
13. Ebrahem Q, et al. Carboxyethylpyrrole oxidative protein modifications stimulate neovascularization: Implications for age-related macular degeneration. Proc Natl Acad Sci U S A 2006;103 (36):13480–13484. [PubMed: 16938854]
14. Manley PW, et al. Anthranilic acid amides: a novel class of antiangiogenic VEGF receptor kinase inhibitors. J Med Chem 2002;45 (26):5687–5693. [PubMed: 12477352]
15. Palm NW, Medzhitov R. Pattern recognition receptors and control of adaptive immunity. Immunol Rev 2009;227 (1):221–233. [PubMed: 19120487]
16. Kawai T, Akira S. Pathogen recognition with Toll-like receptors. Curr Opin Immunol 2005;17 (4): 338–344. [PubMed: 15950447]
17. Shi H, et al. TLR4 links innate immunity and fatty acid-induced insulin resistance. J Clin Invest 2006;116 (11):3015–3025. [PubMed: 17053832]
18. Apetoh L, et al. Toll-like receptor 4-dependent contribution of the immune system to anticancer chemotherapy and radiotherapy. Nat Med 2007;13 (9):1050–1059. [PubMed: 17704786]
19. Kim HS, et al. Toll-like receptor 2 senses beta-cell death and contributes to the initiation of autoimmune diabetes. Immunity 2007;27 (2):321–333. [PubMed: 17707128]
20. Vogl T, et al. Mrp8 and Mrp14 are endogenous activators of Toll-like receptor 4, promoting lethal, endotoxin-induced shock. Nat Med 2007;13 (9):1042–1049. [PubMed: 17767165]
21. Schaefer L, et al. The matrix component biglycan is proinflammatory and signals through Toll-like receptors 4 and 2 in macrophages. J Clin Invest 2005;115 (8):2223–2233. [PubMed: 16025156]
22. Jiang D, et al. Regulation of lung injury and repair by Toll-like receptors and hyaluronan. Nat Med 2005;11 (11):1173–1179. [PubMed: 16244651]
23. Grote K, et al. Toll-like receptor 2/6 stimulation promotes angiogenesis via GMCSF as a potential strategy for immune defense and tissue regeneration. Blood 115(12):2543–2552. [PubMed: 20056792]
24. Zahringer U, Lindner B, Inamura S, Heine H, Alexander C. TLR2 -promiscuous or specific? A critical re-evaluation of a receptor expressing apparent broad specificity. Immunobiology 2008;213 (3–4):205–224. [PubMed: 18406368]
25. Aliprantis AO, et al. Cell activation and apoptosis by bacterial lipoproteins through toll-like receptor-2. Science 1999;285 (5428):736–739. [PubMed: 10426996]

26. Ozinsky A, et al. The repertoire for pattern recognition of pathogens by the innate immune system is defined by cooperation between toll-like receptors. Proc Natl Acad Sci U S A 2000;97 (25): 13766–13771. [PubMed: 11095740]

27. Tan W, et al. An essential role for Rac1 in endothelial cell function and vascular development. FASEB J 2008;22 (6):1829–1838. [PubMed: 18245172]

28. Arbibe L, et al. Toll-like receptor 2-mediated NF-kappa B activation requires a Rac1-dependent pathway. Nat Immunol 2000;1 (6):533–540. [PubMed: 11101877]

29. Mullick AE, Tobias PS, Curtiss LK. Modulation of atherosclerosis in mice by Toll-like receptor 2. J Clin Invest 2005;115 (11):3149–3156. [PubMed: 16211093]

30. Chen J, et al. Akt1 regulates pathological angiogenesis, vascular maturation and permeability *in vivo*. Nat Med 2005;11 (11):1188–1196. [PubMed: 16227992]

31. Feng W, et al. The angiogenic response is dictated by beta3 integrin on bone marrow-derived cells. J Cell Biol 2008;183 (6):1145–1157. [PubMed: 19075116]

32. Mahabeleshwar GH, Somanath PR, Byzova TV. Methods for isolation of endothelial and smooth muscle cells and *in vitro* proliferation assays. Methods Mol Med 2006;129:197–208. [PubMed: 17085813]

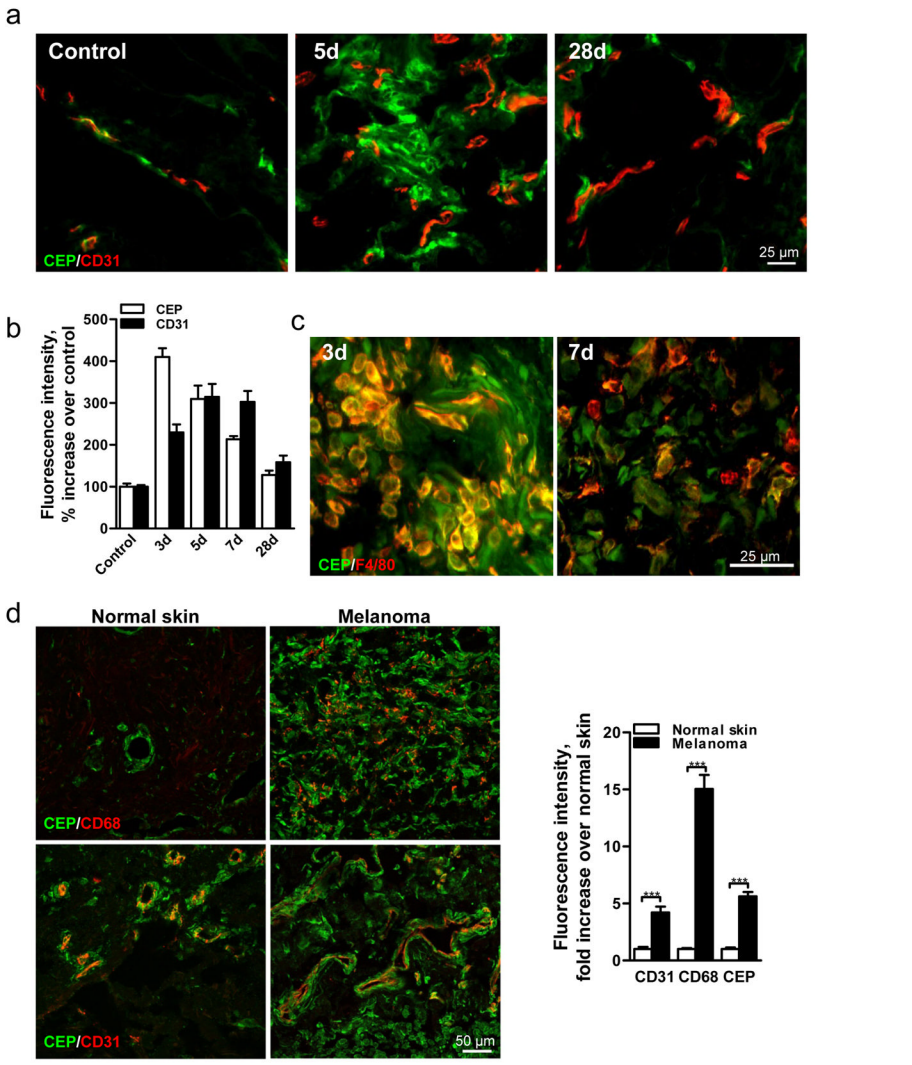

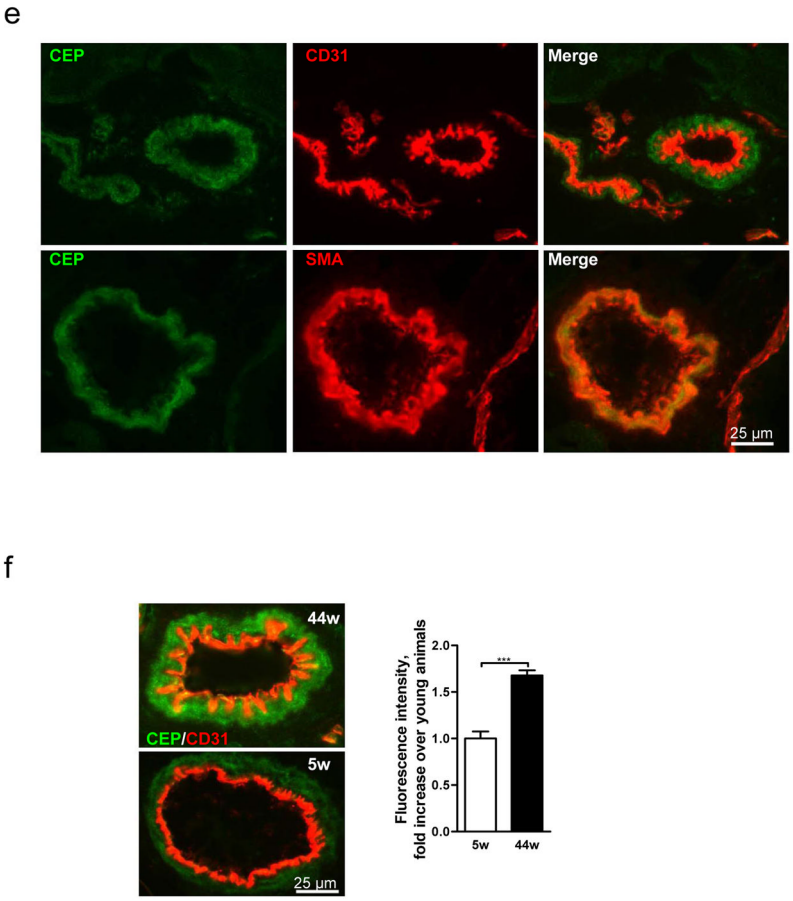

Fig. 1. CEP, an end product of lipid oxidation, is present in wounds, elevated in melanoma and accumulated in aging tissues

a. CEP and CD31 co-staining in normal and wounded skin 5 and 28 days post-injury. **b.** Quantified levels of CEP and CD31, n=5. **c.** F4/80 macrophage marker and CEP distribution in wound tissues 3 and 7 days post-injury**. d.** CEP and CD68 (top) or CEP and CD31 (bottom) presence in human skin and melanoma. Right- quantified levels of CD31, CD68 and CEP, n=8. **e.** CEP and CD31 (top) or CEP and SMA (bottom) distribution in murine skeletal muscle. **f.** CEP and CD31 co-staining in Vastus intermedius sections from 5 and 44 week old mice. Right- CEP quantification, n=4. All values represent mean ± s.e.m. *** $p<0.001$.

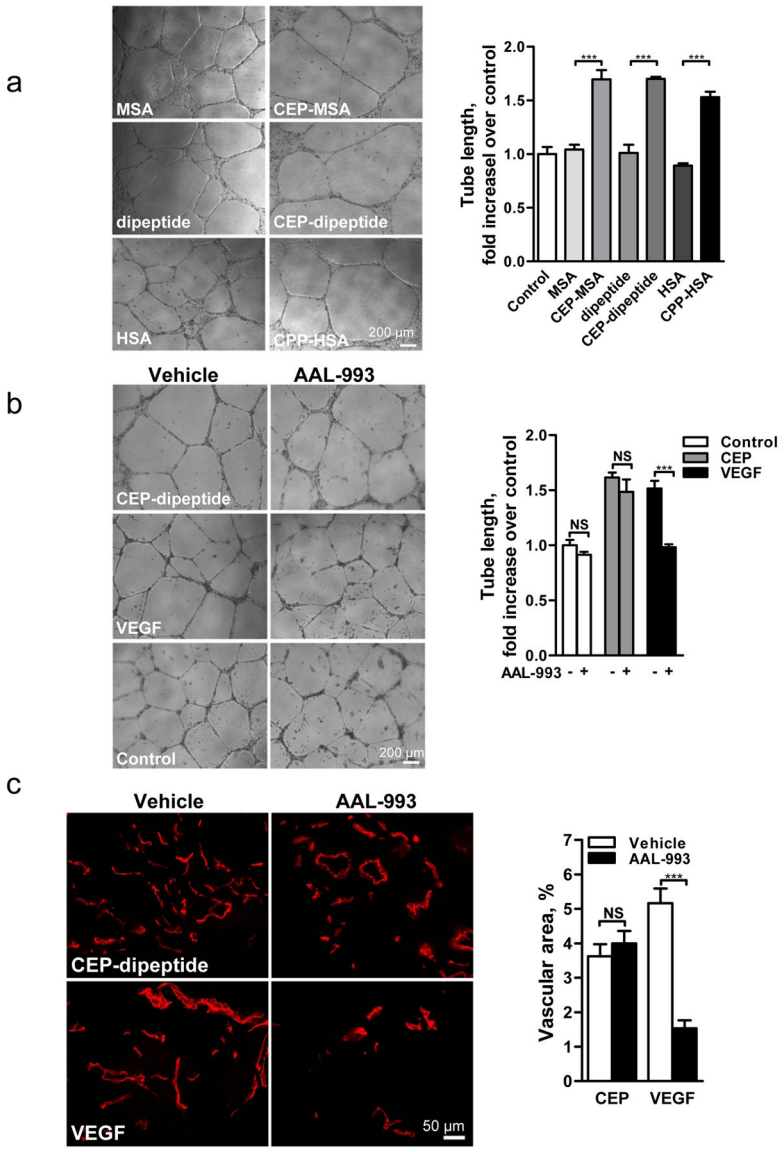

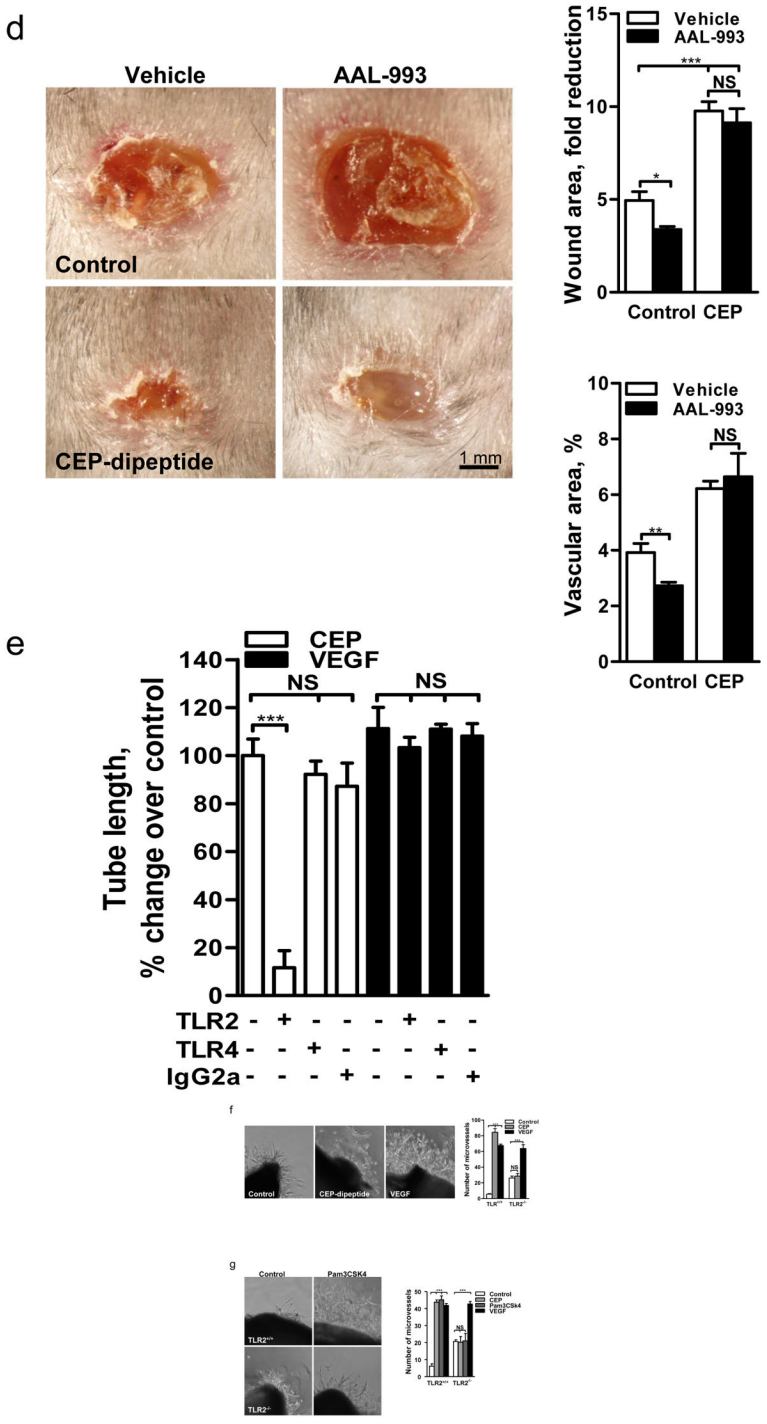

Fig. 2. Proangiogenic effects of oxidized adducts are dependent on pyrrole moiety and are mediated by TLR2 but not VEGFR signaling

a. Images of microvessels in aortic ring assay, treated with pyrrole adducts as indicated. **b.** Effect of AAL-993 on CEP-dipeptide (CEP) and VEGF-stimulated proangiogenic response. Right- assay quantification, n=5. **c.** Growth of CD31 positive blood vessels in matrigel plugs treated as indicated. Right- vascular area quantification, n=5. **d.** Punch wounds treated with CEP-dipeptide and AAL-993, day 6. Right-wound surface areas (top) and vascular areas,

(bottom), n=5. **e.** Quantified tubulogenesis by CEP-dipeptide or VEGF in the presence of blocking anti-TLR2 or anti-TLR4 antibodies, n=4. **f.** $TLR2^{-/-}$ aortic ring cell extrusion in response to CEP-dipeptide or VEGF. Right- microvessel quantification from $TLR2^{+/+}$ and $TLR2^{-/-}$ cultures, n=5. **g.** Images of $TLR2^{+/+}$ and $TLR2^{-/-}$ aortic rings treated with TLR2 ligand Pam3CSK4. Right- assay quantification, n=5. All values represent mean ± s.e.m. * $p<0.05$, ** $p<0.01$ and *** $p<0.001$. NS represents not significant.

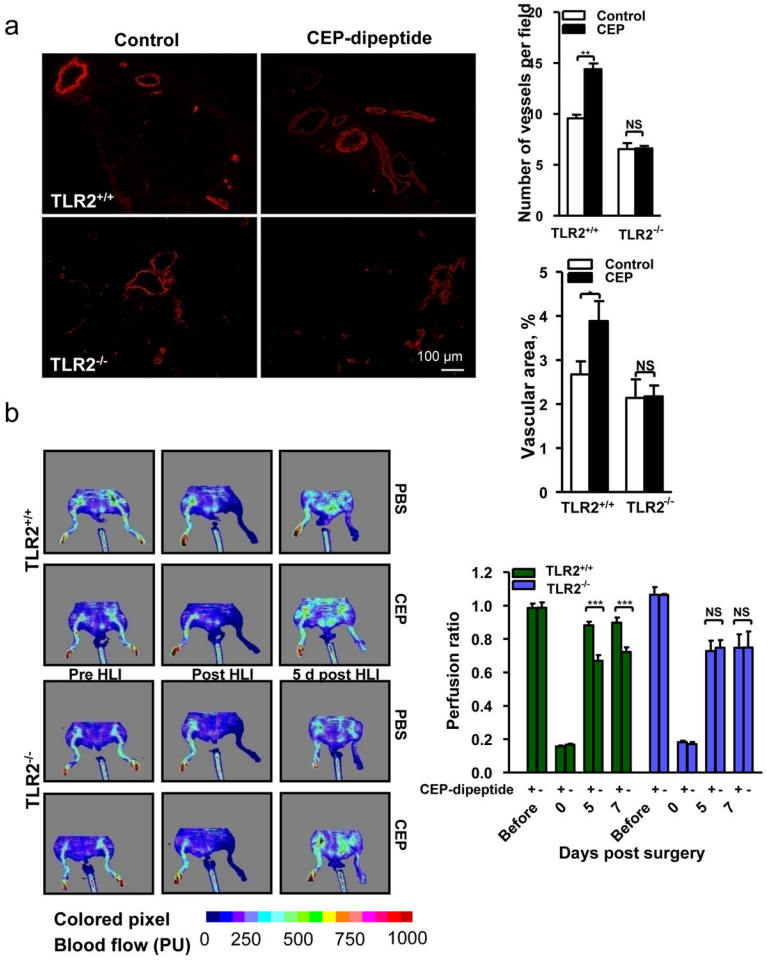

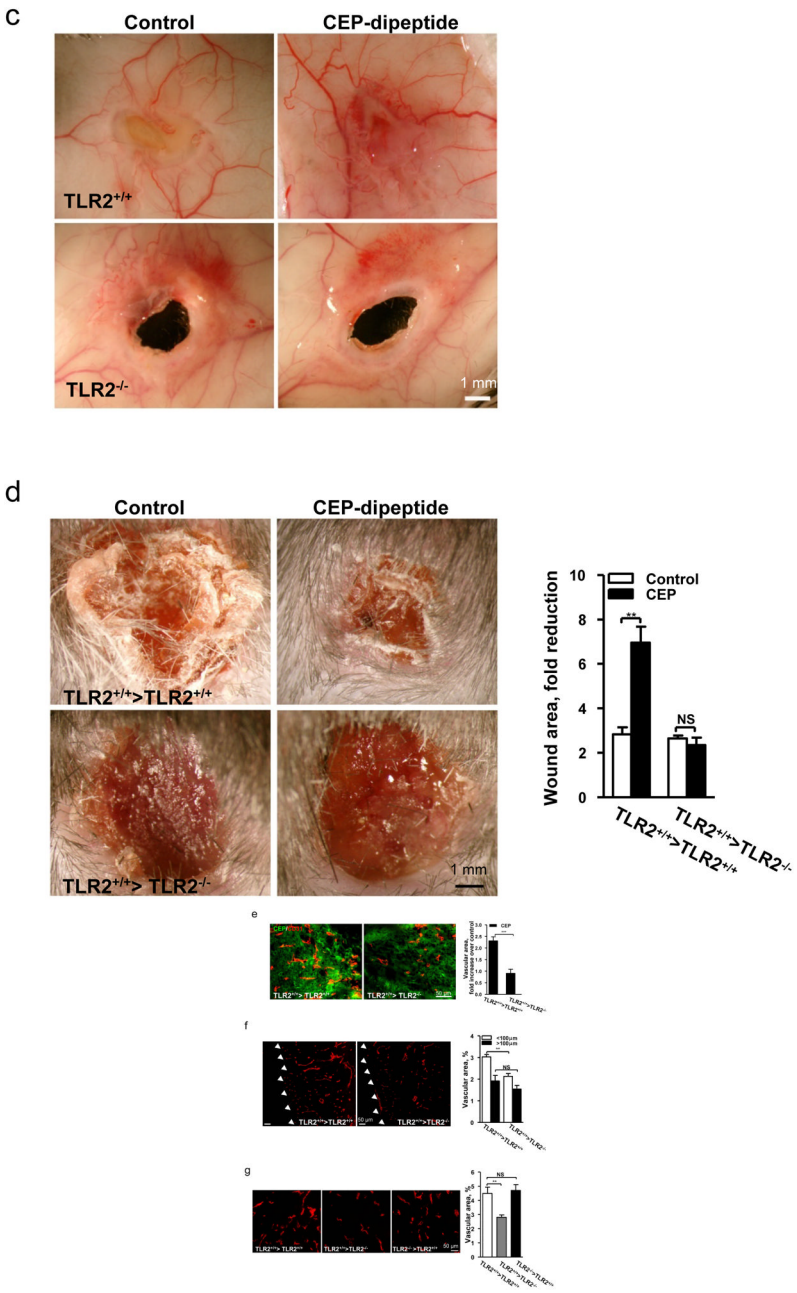

Fig. 3. CEP-induced angiogenesis *in vivo* is mediated by TLR2

a. Vascularization (SMA immunostaining) in hind limbs post-ischemia. Right- of vascular density quantification. Far Right- vascular area quantification, n=6. **b.** Left- perfusion ratio of hind limb blood flow after treatment with CEP, n=8. Right- LDI images. **c.** Images of wound, inner skin flap day 7 post-injury. **d.** Wounds treated with CEP-dipeptide in $TLR2^{-/-}$ and $TLR2^{+/+}$ hosts after $TLR2^{+/+}$ BMT. Right- wound area quantification, n=5. **e.** Vascularization in CEP treated wounds after BMT as indicated. Right- vascular area quantification, n=5. **f.** CD31 staining in wound granulation tissue after BMT. Arrowheads delineate the tissue edge. Right- vascular areas at granulation tissue edge (<100 μm from the outer edge) and deeper areas (>100 μm), n=5. **g.** CD31 positive vasculature in melanoma

allografts, BMT as indicated. Right- vascular area quantification, n=5. All values represent mean ± s.e.m. * $p<0.05$, ** $p<0.01$ and *** $p<0.001$. NS represents not significant.

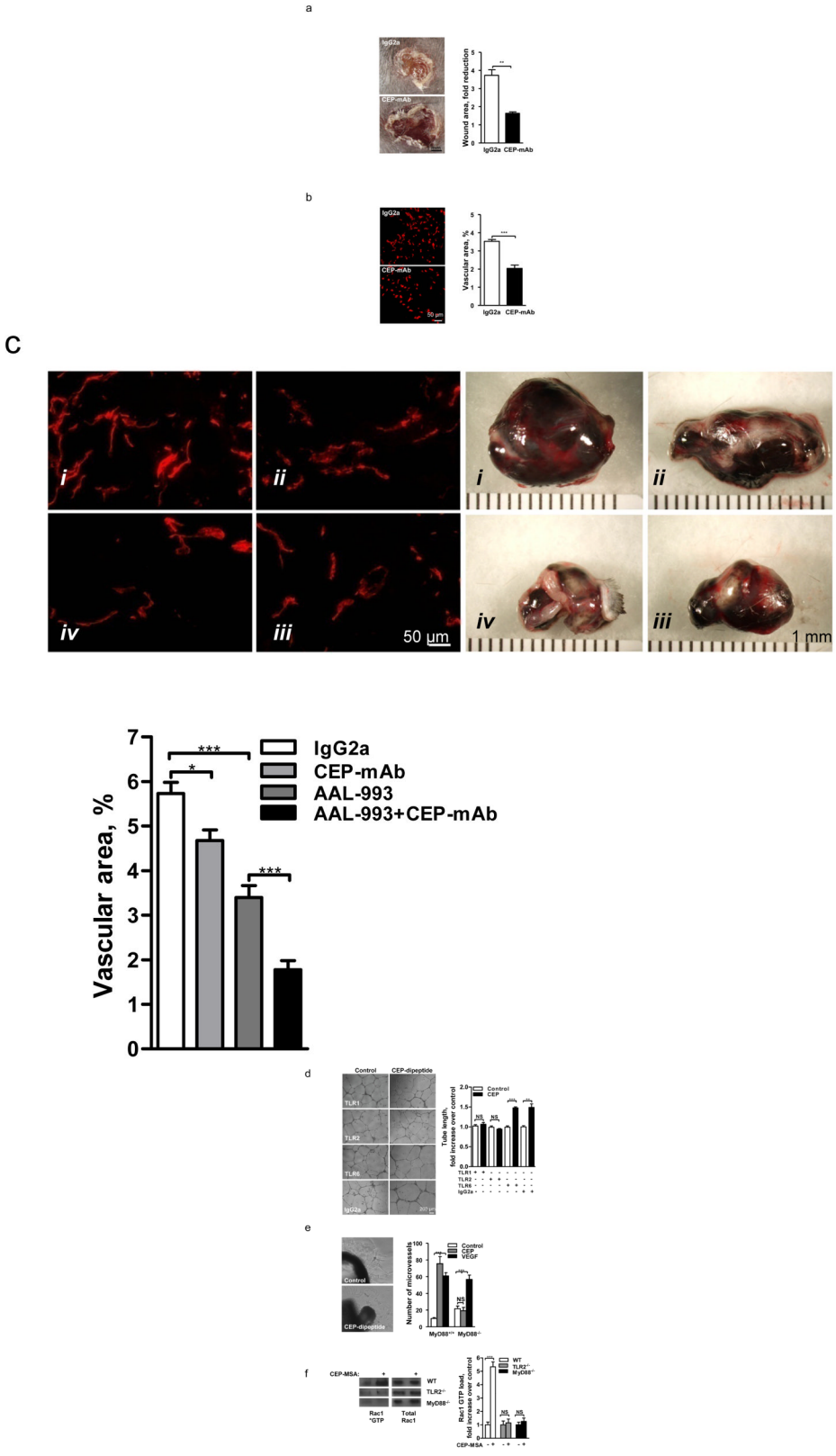

Fig. 4. Endogenous CEP contributes to wound recovery and melanoma vascularization. TLR2-dependent responses to CEP involve MyD88 and Rac1

a. Day 7 post-injury wounds treated with control IgG or anti-CEP blocking antibody. Right-quantified wound area changes, n=5. **b.** CD31-positive wound vasculature. Right-quantified vascular area, n=3. **c.** Melanoma allograft treated with i - control IgG; ii - anti-CEP antibodies; iii - AAL-993; iv - AAL-993 and anti-CEP antibodies. Left- melanoma CD31 immunostaining. Right- tumor size, day 10. Far Right- vascular area, n=4. **d.** CEP-induced tubulogenesis in the presence of control (IgG2a) or anti-TLR-1, -2 or -6 blocking antibodies. Right-tube length quantification, n=5. **e.** Images of $MyD88^{-/-}$ aortic rings treated with CEP-dipeptide. Right- microvessel number in $MyD88^{+/+}$ and $MyD88^{-/-}$ samples, n=5. **f.** Rac1 activation in response to CEP, genotypes as indicated, WT -wild type. Right- assay densitometry, n=3. All values represent mean ± s.e.m. * $p<0.05$, ** $p<0.01$ and *** $p<0.001$. NS represents not significant.